



# Global consumption-based deforestation carbon emissions and regional hotspots: 2001–2015

Dongmei Tang<sup>1</sup>, Yuanzhi Yao<sup>1</sup>, Xia Li\*<sup>1</sup>

<sup>1</sup>School of Geographic Sciences, and Key Lab of Geographic Information Science (Ministry of Education), East China Normal University, Shanghai 200241, PR China

Correspondence to: Xia Li (lixia@geo.ecnu.edu.cn)

**Abstract.** The consumption-based carbon emissions dataset for deforestation is essential for developing effective emission reduction policies by offering an alternative perspective. Although previous studies have provided national-scale data on deforestation emission footprints, the global scale data with detailed and continuous spatial information is still lacking. Here, we created a global consumption-based carbon emissions gridded dataset for deforestation at a 1 km resolution for 2001–2015, integrating spatial data on road networks, deforestation, and forest carbon fluxes with country-level statistics on global trade. Our dataset reveals that trade-related carbon emissions induced by deforestation were 25.3 Gt CO<sub>2</sub>e, constituting 31.0% of global carbon emissions due to deforestation. Additionally, the top 20 countries are responsible for most of the consumption-based carbon emissions which contribute to over 80% of the global total. While high-income countries are responsible for 68.8% of hidden deforestation emissions in trade, the ones in lower-income counties are rising due to the notable consumption in higher-income areas. This new dataset help addresses the previous data gap in consumption-based global deforestation emissions, aiding the formulation of consumer-side emission reduction strategies and expanding the approaches for mitigating carbon emissions due to anthropogenic activities. Datasets are available at <https://doi.org/10.6084/m9.figshare.28091879> (Tang et al., 2024).

## 1 Introduction

Forests typically represent the biotic community with the highest carbon sequestration potential and play a critical role in global climate change mitigation efforts (Cook-Patton et al., 2020). However, over the past two decades, the global land area covered by forests has decreased from 31.6% in 1990 to 30.6% in 2015 (Fao, 2015). Although there has been a recent downward trend in the rate of deforestation, the deforestation continues to occur at an alarming pace. Consequently, deforestation leads to significant carbon emissions, which remained at approximately 1.9 GtC yr<sup>-1</sup> during the period from 2013 to 2022, accounting for 17% of the global total anthropogenic emissions (Friedlingstein et al., 2023). Therefore, effectively managing deforestation holds significant potential for mitigating global carbon emissions.

International trade remains the primary driver of deforestation (Pendrill et al., 2019b; Pendrill et al., 2019a). For instance, large-scale commercial agricultural production, including livestock farming, oil palm, rubber, and cash crops, accounts for



30 40% of tropical deforestation (Wang et al., 2023; Souza Jr, 2023). Previous studies have indicated that 29%-39% of  
deforestation-related emissions are driven by international trade (Pendrill et al., 2019b). Although trade promotes global  
prosperity, it also creates a spatial disconnection between production and consumption (Wiedmann and Lenzen, 2018).  
Consequently, there is increasing recognition that effectively reducing emissions from deforestation requires accounting for  
emissions associated with consumption and implementing policy measures across international supply chains (Pendrill et al.,  
35 2019b; Lambin et al., 2018). The concept of consumption-based deforestation emissions, known as the deforestation  
emissions footprint, describes the deforestation emissions consequences of specific consuming countries.

Mapping global sub-national scale deforestation footprint maps remain challenging due to technical gaps in spatial analysis  
approaches though its significance has been recognized. Previous studies have focused on a handful of countries or country-  
level footprint without considering regional variations within a country (Pendrill et al., 2019b; Pendrill et al., 2019a). This  
40 hampers the accurate calculation of trade and consumption footprints, masking and distorting the causal links between  
consumers' choices and their environmental impacts, especially in countries with significant spatial variability in carbon  
storage conditions (Moran et al., 2020). To address this limitation, some studies have proposed spatially explicit input-output  
models (SMRIO) that use geospatial data for finer-resolution footprint mapping (Hoang and Kanemoto, 2021; Kanemoto et  
al., 2016). Nevertheless, these SMRIO approaches assume proportionality between consumption volumes and production for  
45 each pixel, conducting a within-country analysis that disregards the possibility of exports from specific regions.  
Consequently, when mapping the deforestation emissions footprint, it is challenging to formulate targeted policy measures  
for mitigating carbon emissions from deforestation in specific areas without considering spatial heterogeneity.

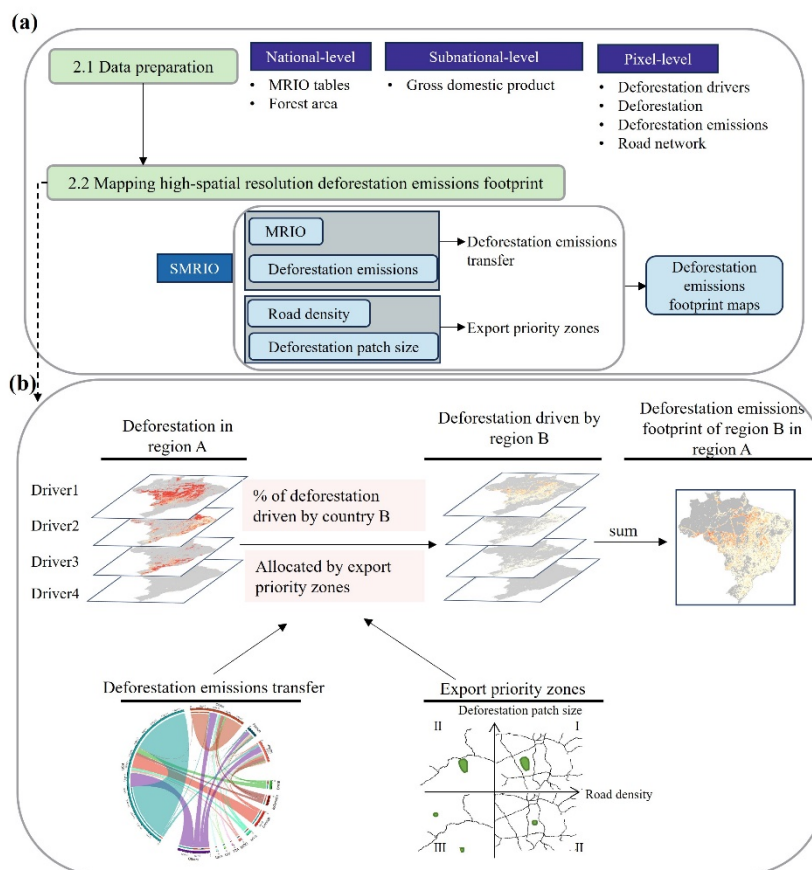
In this study, we developed a global dataset for deforestation emissions footprint with high spatial resolution by enhancing  
the SMRIO method through pixel-level analysis which effectively address the abovementioned technical gaps. By utilizing  
50 geospatial observation data and economic data, we improve the representation of the SMRIO method. Specifically, we  
generate 1 km-resolution maps of deforestation emissions footprints for the period 2001–2015 and identify hotspots driven  
by international consumption. This dataset is, to our knowledge, the first to comprehensively map pixel-level, global  
consumption-based deforestation emissions. The dataset will facilitate the attribution of deforestation emissions  
responsibility to consumers and support recent efforts to eliminate deforestation from supply chains, ultimately aiding in the  
55 development of effective policies to reduce emissions from deforestation.

## 2 Data and Methods

In this study, the SMRIO method for country-level analysis was enhanced by creating priority export zones, enabling the  
mapping of deforestation emissions footprints at a 1 km spatial resolution (Fig. 1). These priority export zones, generated  
from geospatial data such as deforestation and road density maps, were incorporated into the SMRIO model to determine the



60 sequence of regional deforestation exports. Consequently, the deforestation emissions footprint was mapped annually from 2001 to 2015 for 187 countries and regions. A detailed description of the data and methodology is presented in Fig. 1.



65 **Figure 1. (a) Overview of the key steps in mapping pixel-level dataset for deforestation emissions footprint, along with data sources. (b) Illustration of the SMRIO method. The SMRIO method was constructed by combining pixel-level geospatial data with national-level statistical data. The export priority zones were used to enhance the existing method to map the pixel-level deforestation emissions footprint.**

## 2.1 Data preparation

### 2.1.1 The global MRIO tables at national level

70 MRIO tables, widely used for analyzing various environmental footprints, provide a comprehensive representation of the supply and demand of goods and services, including both intra-regional and inter-regional trade (Kanemoto et al., 2016; Lenzen et al., 2018; Liu et al., 2022). In this study, we utilized a simplified version of the Eora MRIO tables, specifically the Eora 26, spanning from 2001 to 2015. The Eora 26 tables represent a time series of global MRIO tables, employing a harmonized 26-sector classification system across 187 countries and regions (Lenzen et al., 2013). These tables allow us to



75 estimate the deforestation footprint associated with specific final demands and the export-oriented volume of deforestation for each country.

### 2.1.2 Pixel-level deforestation, deforestation emissions, and road densities

We obtained the deforestation data from Hansen et al. (2013), which is derived from time-series analysis of Landsat images and is updated annually on Global Forest Watch. In this study, deforestation is defined as the complete removal of tree cover canopy or a stand-replacement disturbance at the scale of Landsat pixels, following Hansen et al. (2013). The deforestation emissions data was obtained from Harris et al. (2021), who also used the annual forest loss data from Hansen et al. (2013), ensuring consistency with our study's basic data. Harris et al. mapped carbon emissions from global forest extent by synthesizing information from over 637,000 ground plots, 707,561 waveform lidar observations, and other satellite data into a spatial forest carbon monitoring framework. To maintain temporal consistency with the deforestation drivers and MRIO tables, we only used deforestation data up to 2015. This pixel-level geo-observation data, which captures spatial heterogeneity, was utilized to spatially distribute the national-level deforestation footprint.

To assign deforestation to different economic sectors, we categorized deforestation based on the intrinsic drivers identified by Curtis et al. (2018). These deforestation drivers were determined using high-resolution (10-km) Google Earth images and a decision tree with nearly 5,000 training sample records of forest change from 2001 to 2015. The drivers of deforestation include commodity-driven deforestation (large-scale deforestation primarily associated with commercial agricultural expansion), shifting agriculture (temporary or permanent deforestation resulting from small- and medium-scale agriculture), forestry (temporary loss due to plantation and natural forest harvesting, including the deforestation of primary forests), wildfire (temporary loss, excluding fire clearing for agriculture), and urbanization (deforestation for urban expansion).

To measure transportation convenience, we utilized road density as a proxy, which was obtained from the Global Roads Inventory Project (GRIP) dataset (Meijer et al., 2018). The GRIP dataset harmonizes approximately 60 geospatial datasets on road infrastructure and provides a global raster of road density at a 5-arcminute resolution (~8 km×8km).

### 2.1.3 The income categories for countries

The income categories, defined by gross national income (GNI) per capita in US dollars, were obtained from the World Bank. These categories include four income levels: Low income (L) for GNI per capita less than \$1,006, Lower-middle income (LM) for GNI per capita between \$1,006 and \$3,975, Upper-middle income (UM) for GNI per capita between \$3,976 and \$12,275, and High income (H) for GNI per capita greater than \$12,275.



## 2.2 Mapping high-spatial resolution deforestation emissions footprint

### 2.2.1 Multi-regional input-output model (MRIO)

The MRIO method is widely used to examine the connections between economic activities and natural resources, as well as their environmental impacts (Tang et al., 2021; Lenzen et al., 2018). MRIO tables describe the equilibrium of supply and demand among sectors in various regions, providing detailed information on the flows of goods and services both within and between economies. This balance of supply and demand in MRIO tables can be expressed as Eq. (1):

$$X = T + Y, \quad (1)$$

where  $X = [x_i^r]$  denotes total output of sector  $i$  in region  $r$ ;  $T = [z_{ij}^{rs}]$  is the intermediate input-output from sector  $i$  in region  $r$  to sector  $j$  in region  $s$ ;  $Y = [y_i^{rs}]$  is the final demand in region  $s$  supplied by sector  $i$  in region  $r$ . When the technical coefficient  $A$  is introduced, Equation (1) can be reformulated as follows:

$$X = (I - A)^{-1} \times Y, \quad (2)$$

where  $A = T/X = [a_{ij}^{rs}]$  represents the amount of input of sector  $i$  in region  $r$  to satisfy the unit value increase in output of sector  $j$  in region  $s$ ;  $I$  is the identity matrix;  $(I - A)^{-1} = [b_{ij}^{rs}]$  is the Leontief inverse matrix (L), which represents the gross output from sector  $i$  in region  $r$  to satisfy one monetary unit of final demand in sector  $j$  of region  $s$ . To establish a connection between the monetary output and deforestation, a crucial step is to determine the direct deforestation intensity  $f$ , which is calculated as:

$$f = Q/X, \quad (3)$$

where  $f$  is the amount of deforestation per monetary unit of sectoral outputs;  $Q = [q_j^s]$  is the deforestation area of sector  $j$  in region  $s$ , which is also known as deforestation satellite account.

Notably, wildfires caused by natural or human activities were excluded from this analysis since they are not directly associated with economic activities. Our focus was on economic-related deforestation drivers such as commodity-driven deforestation, shifting agriculture, and forestry, which correspond to the agricultural sector in the Eora26 tables, as well as urbanization, which corresponds to the construction sector. Additionally, commodity-driven deforestation includes activities driven by mining or energy infrastructure, corresponding to the mining and quarrying sector. In cases where a single deforestation driver corresponds to multiple sectors, the deforestation area was allocated proportionally to the added value of each sector (Hoang and Kanemoto, 2021; Kanemoto et al., 2016).

Thus, the transfer of deforestation between regions driven by final demand can be calculated by

$$E = \hat{f}Ly, \quad (4)$$

where  $E$  is the deforestation transfer matrix;  $\hat{f}$  is a diagonal matrix of  $f$ ;  $y$  is the final demand.



130 **2.2.2. Export priority zones**

The SMRIO model, originating from the MRIO method, utilizes fine-scale geospatial data to allocate consumption-driven deforestation emissions to specific grids. We further enhanced the SMRIO method by incorporating priority export zones, allowing the mapping of deforestation emissions footprints at a 1 km resolution as follows:

$$F_h^{sr} = \begin{cases} R1_h^r \frac{\sum_i f_i^r \sum_j L_{ij}^r y_j^{ts}}{\sum_i d1_{hi}^r} & \text{if } \sum_j L_{ij}^r y_j^{ts} < \sum_i d1_{hi}^r \\ R1_h^r + R2_h^r \frac{(\sum_i f_i^r \sum_j L_{ij}^r y_j^{ts} - \sum_i d1_{hi}^r)}{\sum_i d2_{hi}^r} & \text{if } \sum_i d1_{hi}^r < \sum_i f_i^r \sum_j L_{ij}^r y_j^{ts} < \sum_i d2_{hi}^r \\ R1_h^r + R2_h^r + R3_h^r \frac{(\sum_i f_i^r \sum_j L_{ij}^r y_j^{ts} - \sum_i d1_{hi}^r - \sum_i d2_{hi}^r)}{\sum_i d3_{hi}^r} & \text{if } \sum_i d2_{hi}^r < \sum_i f_i^r \sum_j L_{ij}^r y_j^{ts} < \sum_i d3_{hi}^r \end{cases}, \quad (5)$$

135  $F^s = \sum_{hr} F_h^{sr}$ . (6)

where  $F^s$  denotes deforestation emissions footprint map of country  $s$  in the world;  $R$  denotes map of deforestation emissions for each of  $h = 1$  to 4 drivers, and  $R1_h^r$ ,  $R2_h^r$ , and  $R3_h^r$  are maps of deforestation emissions caused by driver  $h$  in the first, second and third priority export areas in country  $r$ , respectively.  $d$  denotes deforestation area, and  $d1$ ,  $d2$ , and  $d3$  are deforestation areas in the first, second and third priority export areas in country  $r$ . The embodied deforestation emissions term ( $fLy$ ) and  $d$  are in absolute values;  $i$  and  $j$  represent the sectors of origin and destination, and  $r$  and  $s$  denote the countries of production and final sale;  $t$  is the country of final demand.

The international demand for export-oriented agricultural products is widely recognized as a significant driver of deforestation (Defries et al., 2010). Profit-driven export trade in agricultural and forestry commodities tends to be concentrated in regions with extensive farmland (Friis and Nielsen, 2019) and well-connected locations (Verburg et al., 2011). Consequently, deforestation often occurs in large patches, primarily in easily accessible areas. Export priority zones are identified to estimate deforestation associated with potential exports or domestic consumption by examining the size of deforestation patches and road density (Meijer et al., 2018). Our assumption is that higher road density and larger deforested patch sizes indicate a greater likelihood of export-oriented deforestation. The size of deforested patches was calculated using the landscape pattern index and standardized to a range between 0 and 1 through min-max transformation within each country. We set the threshold for the size of deforested patches at 0.5, while the threshold for road density was 100 m/km<sup>2</sup>, following Sun et al. (2020). As a result, three export priority zones were identified (Table 1).

**Table 1. the definition of three export priority in this study**

Export priority	Definition
<b>First</b>	Size > 0.5 And Density > 100
<b>second</b>	(Size > 0.5 And Density < 100) or (Size < 0.5 And Density > 100)
<b>Third</b>	Size < 0.5 And Density < 100



Notes: Size denotes the size of deforested patches; Density denotes the road density (unit:  $\text{m}/\text{km}^2$ ).

155 If the deforestation area caused by foreign consumption in a specific region exceeds the deforestation area in the first export  
priority zone, the remaining deforestation area is proportionally distributed among the second priority export zone based on  
its deforestation area proportion (which is less than 1). If this proportion exceeds 1, the remaining deforestation is further  
distributed to the third priority export zone according to the deforestation area proportion in the third export priority zone.  
Conversely, deforestation driven by domestic consumption is assigned to priority zones in reverse order.

### 3 Results

#### 160 3.1 Consumption-based deforestation emission footprint between 2001–2015

We estimated the consumption-based deforestation emission associated with dominant anthropogenic activities worldwide  
for the period 2001–2015 using the SMRIO model. During this period, global deforestation averaged 15.8 million hectares  
per year, resulting in emissions of 81.4 Gt  $\text{CO}_2\text{e}$ . Notably, 25.3 Gt  $\text{CO}_2\text{e}$  of these emissions were embodied in trade,  
accounting for 31.0% of the world's deforestation emissions. Regionally, the highest deforestation emission footprints were  
165 observed in Latin America, Southeast Asia, and the United States (Fig. 2). Over the time series, except for Latin America  
and the United States, all regions experienced consistent increases in deforestation emissions footprint, with the most  
significant rises occurring in Southeast Asia and Sub-Saharan Africa.

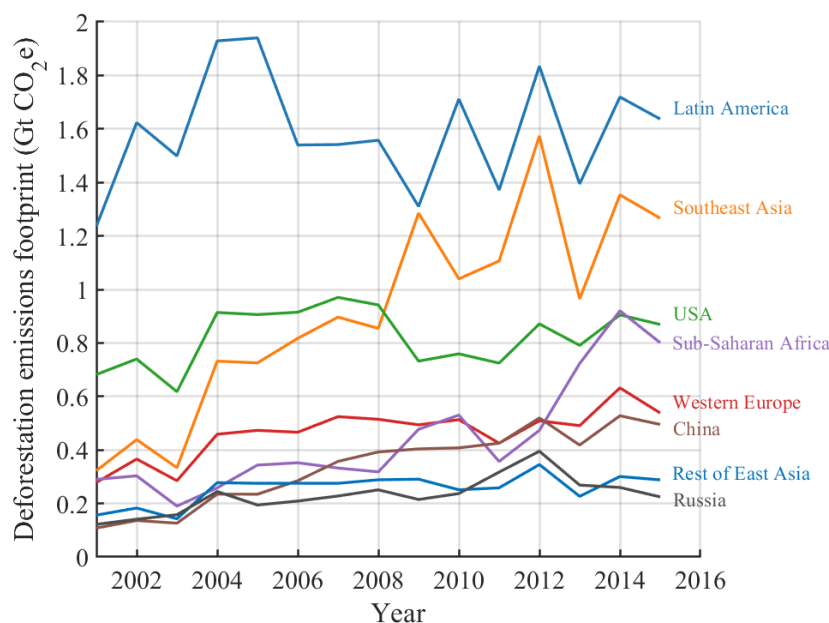
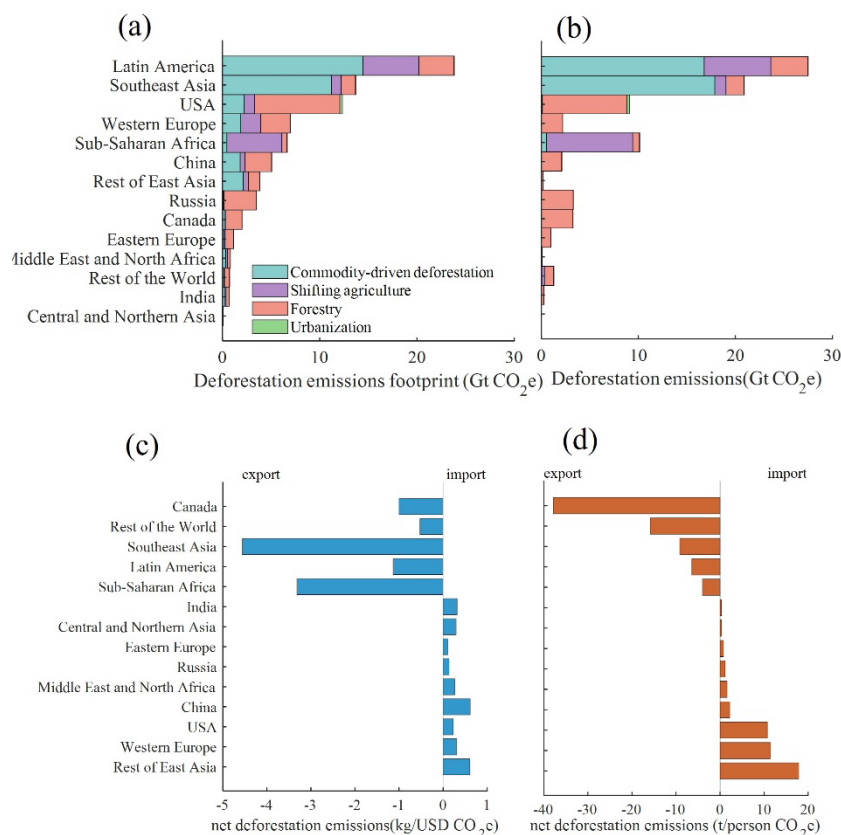


Figure 2. Deforestation emissions footprint in different regions worldwide, 2001–2015.



170 Cumulative deforestation emissions from 2001 to 2015 are further analyzed by deforestation drivers, examining both  
consumption- and production-based deforestation emissions across various global regions (Fig. 3). From the consumer  
perspective, Latin America and Southeast Asia exhibit significant emissions footprints from commodity-driven deforestation.  
In contrast, the United States, China, Russia, and Canada shows substantial contributions from forestry activities. Sub-  
Saharan Africa demonstrates the highest proportion of emissions footprints from shifting agriculture (Fig. 3a). On the  
175 production side, Latin America and Southeast Asia are the leading contributors to deforestation emissions, with a large  
proportion of emissions footprints resulting from commodity-driven deforestation. In the United States, Western Europe,  
China, and other regions, the primary driver of deforestation emissions is forestry, which is relatively singular compared to  
the more diverse drivers on the consumption side (Fig. 3b). Countries that import more trade-based deforestation emission  
than they export are net deforestation emission importers, and vice versa for exporters. There is a striking division between  
180 the world's top ten net importers and net exporters of deforestation emissions. The data show that the United States, Europe,  
and China are the main importers of deforestation emissions, while Southeast Asia, Sub-Saharan Africa, and Canada are the  
main exporters. As illustrated in Fig. 3c, Southeast Asia and Sub-Saharan Africa are the largest exporters of deforestation  
emissions per unit of GDP, whereas China and Rest of East Asia are the largest importers. Figure 3d shows that on a per  
capita basis, the Rest of East Asia, Western Europe, and the USA are major net importers, while Canada and Southeast Asia  
185 are the largest exporters of deforestation emissions per capita.





**Figure 3. Cumulative deforestation emissions in various regions worldwide, 2001–2015: (a) deforestation emissions footprint under different driving forces, (b) deforestation emissions under different driving forces, (c) net import of deforestation emissions per unit GDP, and (d) net import of deforestation emissions per capita.**

190 We analysed consumption- and production-based deforestation emissions in top countries and found that these emissions are primarily concentrated in a few nations (Fig. S1). The consumption- and production-based deforestation emissions from the top 20 countries account for more than 80% of global deforestation emissions. These emissions are mainly driven by commodity-driven deforestation and forestry activities. Specifically, the USA, Indonesia and Brazil are the top three consumers and producers of deforestation emissions. In Indonesia and Brazil, deforestation emissions are predominantly driven by commodity-driven deforestation activities, while in the USA, they are mainly driven by forestry. Most of the top

195 importers of deforestation emissions are high-income countries, whereas most of the top exporters are low- and middle-income countries (Fig. S2). Among the net importers, the net imported deforestation emissions range from 0.4 Gt CO<sub>2</sub> e to 3.3 Gt CO<sub>2</sub> e. The US was the largest net importer, with imports about seven times greater than Spain, the tenth-largest importer. The main drivers of deforestation in these importing countries are commodity-driven deforestation, shifting

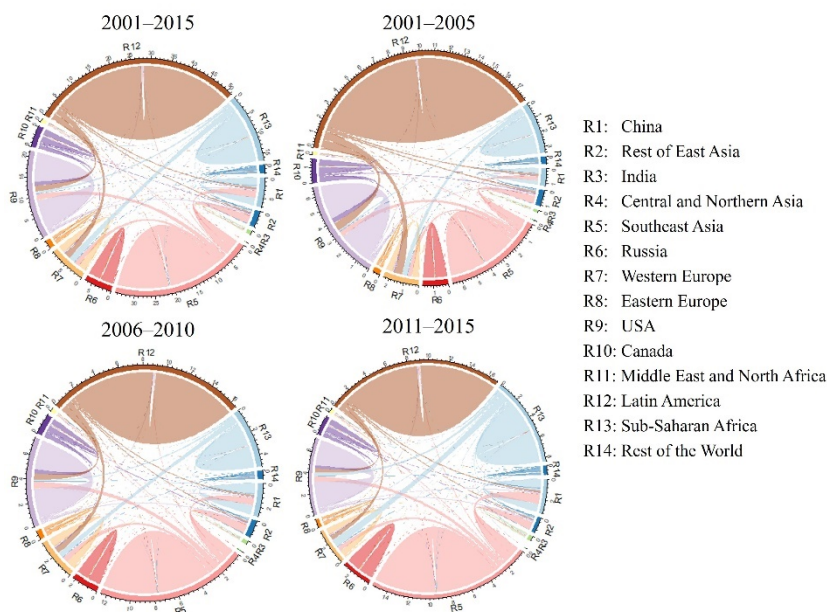
200 agriculture, and forestry. Top countries import large amounts of deforestation emissions driven primarily by commodity-driven deforestation. Among the net exporters, the net exported deforestation emissions range from 0.4 Gt CO<sub>2</sub> e to 4.9 Gt



CO<sub>2</sub> e. Indonesia has the highest exported deforestation emissions, about twelve times larger than those exported by Myanmar. Commodity-driven deforestation emissions are mainly exported from Indonesia, Brazil, Malaysia, and Bolivia, where the economic benefit from cash crops like rubber and palms oil drive significant deforestation. Shifting-agriculture-driven deforestation emissions are primarily exported from Madagascar, Cote d'Ivoire, and DR Congo, while forestry-driven deforestation emissions are mainly exported from Canada.

### 3.2 Embodied deforestation emissions between different regions

We analysed the embodied deforestation emissions between different regions during the period 2001–2015, 2001–2005, 2006–2010, 2011–2015 (Fig. 4). Over the entire period from 2001 to 2015, the United States and Western Europe exhibited the largest hidden trade flows of deforestation emissions, primarily originating from Latin America and Southeast Asia, as well as Latin America and Africa, respectively (Fig. 4a). Additionally, the Rest of East Asian and China showed a significant proportion of deforestation emissions imports, mainly sourced from Southeast Asia during this period (Fig. 4a). Examining the three sub-periods separately, we observed a shift in the regional contributions to global deforestation emissions. From 2001–2015, and then from 2006 to 2010, and finally from 2011 to 2015, Latin America's share of global deforestation emissions decreased, while the shares from Southeast Asia and Africa increased. Notably, there is an increasing trend in the transfer of deforestation emissions from Africa to the United States and Western Europe. Conversely, the deforestation emissions transferred from Latin America to the United States and Western Europe are decreasing (Fig. 4b–4d).



220 **Figure 4. Trade flows of embodied deforestation emissions in various regions worldwide. (a). trade flows of embodied deforestation emissions, 2001–2015. (b). trade flows of embodied deforestation emissions, 2001–2005. (c). trade flows of embodied deforestation emissions, 2006–2010. (d). trade flows of embodied deforestation emissions, 2011–2015.**



We also analyzed the flows of deforestation emissions between these top countries (Fig. S3). Indonesia, Brazil, and Malaysia are the top three exporters of deforestation emissions, accounting for 41.0% of the world's embodied deforestation emissions. This is mainly due to the significant carbon emissions resulting from tropical deforestation. Specifically, deforestation emissions from Indonesia, the largest deforestation emissions exporter, account for 20.1% of the world's deforestation emissions and mainly flow to the USA, Japan, China, and South Korea. Brazil, as the second-largest exporter, accounts for 12.3% of the world's embodied deforestation emissions, with its emissions mainly flowing to the USA and China. The USA, the largest importer of deforestation emissions, accounts for 20.1% of the world's embodied deforestation emissions, importing mainly from Canada, Indonesia, Brazil, and Malaysia. Japan, the second largest importer, accounts for 10.7% of the world's deforestation emissions, with most of its imports coming from Indonesia.

We further analyzed the flows of deforestation emissions embodied in international trade among countries with different income level over various periods (Fig. 5). The analysis shows that the lower the income level, the less deforestation emissions are embodied in international trade of goods and services. Specifically, 68.6% of deforestation emissions embodied in international trade originate from middle-income countries, while high- and low-income countries contribute 21.2% and 10.2%, respectively. Additionally, 68.8% of deforestation emissions embodied in international trade are destined for high-income countries (Fig. 5a). Dividing the period 2001 to 2015 into three sub-periods (2001–2005, 2006–2010, and 2011–2015), we observed significant changes in embodied deforestation emissions between countries with different income level. For instance, deforestation emissions from upper-middle income countries to high-income countries decreased, while imports from low - and lower-middle-income countries increase. For both low - and lower-middle-income countries, deforestation emissions export to upper-middle-income and high-income countries tended to increase.

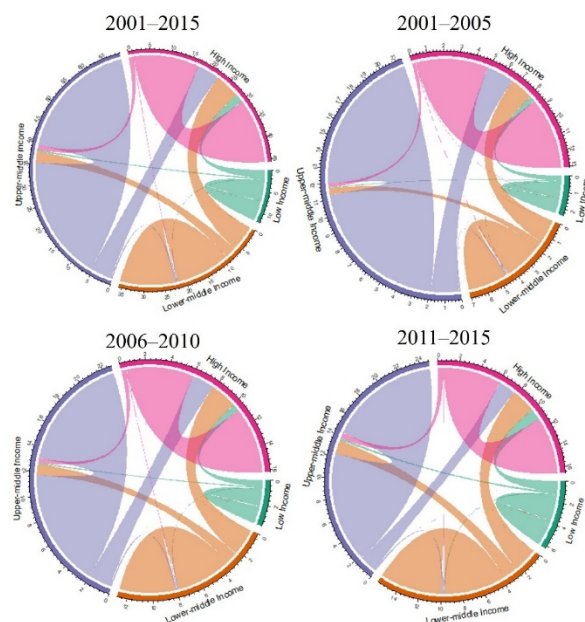


**Figure 5. Trade flows of embodied deforestation emissions in countries with different income level. (a). trade flows of embodied deforestation emissions, 2001–2015. (b). trade flows of embodied deforestation emissions, 2001–2005. (c). trade flows of embodied deforestation emissions, 2006–2010. (d). trade flows of embodied deforestation emissions, 2011–2015.**

245 Top countries of embodied deforestation emissions were divided into four group based on net forest change and imported  
deforestation emissions (Fig. 6). Group I, consisting mostly of high-income countries, experienced net forest gain and net  
imported deforestation emissions. These countries consumed more products with embodied deforestation emissions imported  
from other countries, converting their forests into net gains. For instance, the USA and Japan imported 3.3 Gt and 2.7 Gt  
CO<sub>2</sub> e of net deforestation emissions, respectively, while, their forests increased by 6.0 M ha and 0.1 M ha, respectively.  
250 Because the USA and Japan have strict environmental protection policies, they import products with embodied deforestation  
emissions from other countries. China, a developing country in group I, imported fewer embodied deforestation emissions  
than the USA and Japan but experienced more forest gains due to its commitment to afforestation. Group III, comprising  
mainly low- and middle-income countries, saw net forest loss and net exported deforestation emissions. Those countries  
exported products with embodied deforestation emissions to other countries, leading to net forest loss. For example,  
255 Indonesia and Brazil exported 4.9 Gt and 2.4 Gt CO<sub>2</sub> e of net deforestation emissions, respectively, while their forests  
decreased by 6.1 M ha and 43.3 M ha, respectively. Due to less stringent environmental protection policies and favourable  
climate conditions for cash crops. Indonesia and Brazil face significant deforestation driven by economic benefits. Countries  
in group I exacerbate environmental problems in group III by consuming products with embodied deforestation emissions  
from group III countries. Therefore, it is essential for countries in group I to support environmental protection efforts in  
260 group III countries.

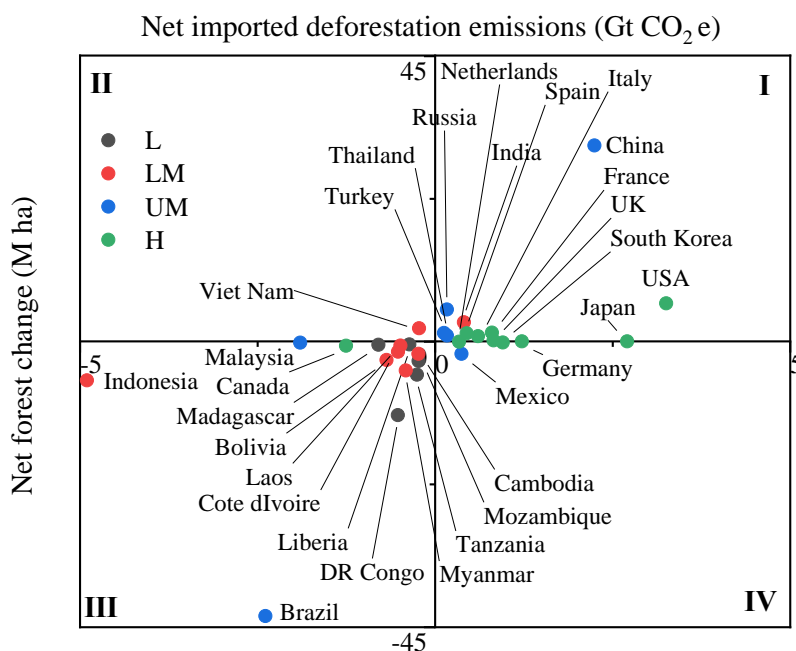
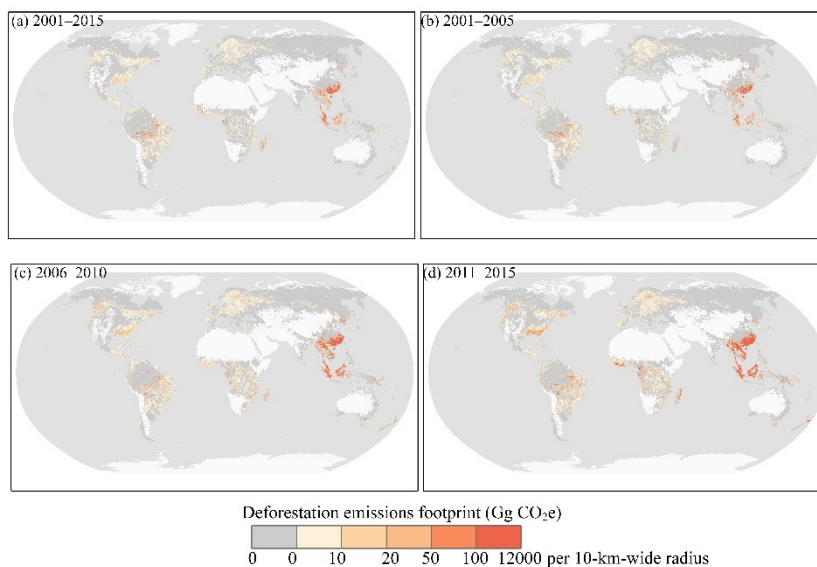


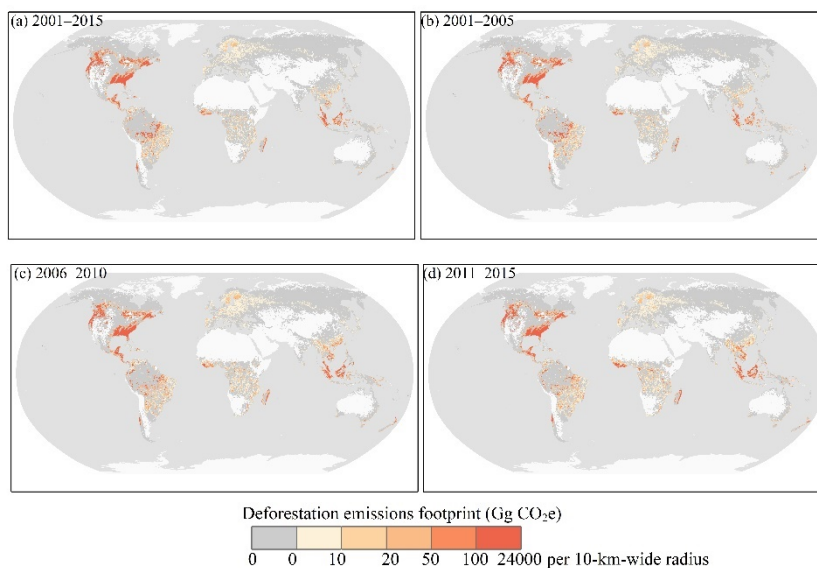
Figure 6. Net forest change and deforestation emissions from top countries, 2001–2015.

### 3.3 Hotspots of deforestation emissions footprint

The new dataset, produced by the improved SMRIO model, well represent the spatial distribution of deforestation emissions footprints. Figure 7 and 8 illustrate the 15-year and three 5-year cumulative deforestation emissions footprints of the USA and China, the world's largest net importers of deforestation emissions. The deforestation emissions induced by consumption in the USA are widely distributed, primarily occurring in domestically and in countries throughout Southeast Asia, especially Indonesia and Malaysia. Additionally, significant emissions footprints are observed in Brazil, particularly in the Amazon Plain, and in several coastal countries in West Africa, such as, Côte d'Ivoire and Liberia, as well as in Eastern Madagascar and Chile. In contrast, China's deforestation emissions footprints are concentrated in North China and extend to Southeast Asia, particularly Indonesia and Malaysia, as well as to Central and western Africa, including Gabon and Cameroon.



**Figure 7. Deforestation emissions footprint driven by the USA, (a) 2001–2015, (b) 2001–2005, (c) 2006–2010, (d) 2011–2015.**



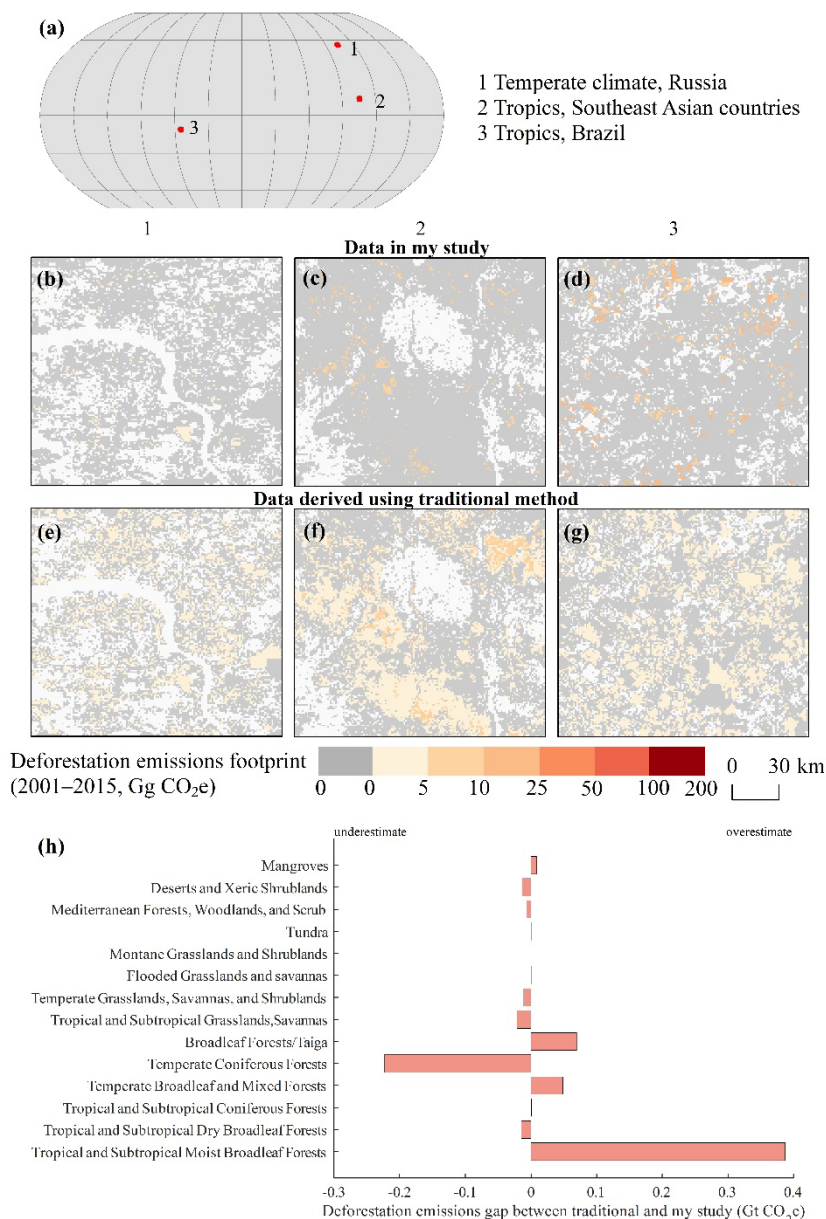
**275 Figure 8. Deforestation emissions footprint driven by China, (a) 2001–2015, (b) 2001–2005, (c) 2006–2010, (d) 2011–2015.**

We compared the distribution of hotspots of deforestation emissions footprints dataset in this study with those derived using traditional method (Fig. 9). As shown in the Fig. 9, the hotspot map from the traditional method displays a larger distribution because it assumes that export-oriented deforestation come from all deforestation regions. Conversely, in this research, regions were divided according to the export-likelihood index, resulting in a relatively smaller range of deforestation





280 emissions footprints. Specifically, for the U.S. deforestation emissions footprint, the traditional method introduced biases in  
 estimating deforestation emissions across different bioregions (Fig. 9h). For instance, it significantly underestimated  
 deforestation emissions in areas of Temperate Coniferous Forests, while overestimating them in areas of Tropical and  
 Subtropical Moist Broadleaf Forests.



285 **Figure 9. Deforestation emissions footprint hotpot from 2001–2015 compared with dataset derived from tradition method.**



## 4 Discussions

### 4.1 Significance of mapping deforestation emissions embodied in international trade

Deforestation emissions are a significant source of greenhouse gases, making large-scale accurate accounting crucial for mitigating these emissions. However, at this stage, there is a lack of fine-scale consumption-based deforestation emissions inventories. In this study, we utilized an improved SMRIO model to map the global 1 km deforestation emission footprint from 2001 to 2015, accounting for consumption-based deforestation emissions. During this period, global deforestation averaged 15.8 million ha yr<sup>-1</sup>, a figure comparable to Fao (2020) statistics. The associated deforestation emissions amounted to 81.4 Gt CO<sub>2</sub>e. Our results reveal that 25.3 Gt CO<sub>2</sub>e of these deforestation emissions were embodied in trade, accounting for 31.0% of global deforestation emission. The share is slightly higher than the land-use emissions share (27%, as reported by Hong et al. (2022)) and the fossil fuel emissions share (23-30%, as stated by Wiedmann and Lenzen (2018)). Hidden land-use and fossil fuel emissions from global trade are critical concerns for climate change mitigation (Hong et al., 2022; Yang et al., 2020; Wiedmann and Lenzen, 2018; Kanemoto et al., 2016). Our findings suggest that deforestation emissions hidden in trade should also be given serious attention. Therefore, to effectively achieve Reducing Emissions from Deforestation and Forest Degradation (REDD), it is necessary to accurately account for emissions from consumption-based deforestation (Pendrill et al., 2019b; Lambin et al., 2018).

### 4.2 Comparisons with other datasets

To date, several deforestation footprint datasets are available (Pendrill et al., 2019b; Henders et al., 2015). However, these datasets have significant limitations. For instance, they are confined to tropical forests (Henders et al., 2015) or use accounting methods that do not fully capture detailed deforestation emissions (Pendrill et al., 2019b). Furthermore, their accounting is based on national scales, failing to reflect regional heterogeneity in deforestation emissions. The existing global-scale deforestation footprint data, derived from SMRIO model, can address the scale problem. However, these data distribute all footprints uniformly throughout the study area, ignoring spatial heterogeneity (Hoang and Kanemoto, 2021; Yang et al., 2020). In this study, our data overcame these limitations by introducing export priority areas, creating a more accurate deforestation emission dataset. Our findings indicate that the data produced by the traditional SMRIO model often overestimates or underestimates deforestation emissions footprints in different ecological zones. Additionally, datasets based on national scales do not account for intra-country variations in deforestation footprints. We used deforestation emissions data from Harris et al. (2021), which is consistent with the annual forest loss data of Hansen et al. (2013). This spatially detailed geographic data allows us to show the spatial heterogeneity of deforestation emissions more precisely and calculate the deforestation emission footprint in greater detail.





### 315 **4.3 Implication for reducing emissions from deforestation**

Latin America, the United States, and Southeast Asia are the largest consumers of deforestation emissions, primarily driven by commodity-driven deforestation and forestry activities. Conversely, Latin America, Southeast Asia, and Sub-Saharan Africa are the largest producers of these emissions. Among producers, lower-middle-income and upper-middle-income countries are the main sources, contributing to 70.2% of global deforestation emissions. Notably, a significant proportion of these deforestation emissions is driven by foreign consumption. For consumers, upper-middle-income and high-income countries are the primary destinations for deforestation emissions, accounting for 41.5% and 35.5%, respectively, of the global total. The higher the income level, the greater the reliance on imported deforestation emissions to meet domestic demand. While this trade can enhance regional prosperity, it also exacerbates environmental pollution in the producer countries. Our dataset illustrates that poorer countries disproportionately bear the burden of deforestation emissions for the developed world. This disparity arises because high-income countries, with more restrictive environmental policies, tend to import forest-related products from lower-income countries with less stringent regulations (Kastner et al., 2011). Kastner et al. (2011) also found that many developed countries restore their own forests by importing wood products. Thus, to effectively reduce deforestation emissions within the context of national trade, it is effective to strengthen policy communication from the production and consumption sides and improve the supply chain to reduce deforestation emissions (Lambin et al. 2018).

### 335 **4.4 Limitations and uncertainties**

This study aims to produce a global fine-scale dataset of deforestation emissions footprint during period 2001–2015. However, it is necessary to address the uncertainties of these datasets before using them. First, due to the lack of detailed trade chain data, we cannot distinguish the specific export destinations of each region (Yang et al., 2020). Consequently, this study assumes that the likelihood of export to each region is the same, consistent with previous research (Yang et al., 2020). Second, this study only considers economic-related deforestation emissions and excludes wildfire emissions, as this driver cannot be linked to economic activity. For further improvements, we call for traceable and transparent supply chain information to enable more accurate consumption-based carbon emissions dataset for deforestation. Third, the timeliness of this dataset is constrained by the input–output model, whose significant limitations is the lengthy time lag in data preparation (He et al., 2022). Fortunately, other underlying data on which the dataset depends, such as satellite-based deforestation data and its drivers, are updated promptly (Hosseiny et al., 2024; Liu et al., 2025). Once the input-output databases are updated, our dataset can be readily extended to incorporate more recent years.



## 5 Data availability

345 Datasets are available at <https://doi.org/10.6084/m9.figshare.28091879> (Tang et al., 2024). Data are in TIFF format.

## 6 Conclusions

The proportion of consumption-driven carbon emissions for deforestation is comparable to that of consumption-driven fossil fuel carbon emissions, highlighting the need to reduce these emissions. However, there is still a lack of detailed global datasets on carbon emissions for deforestation. This study is the first to generate time-series gridded datasets for consumption-based deforestation emissions from 2001 to 2015. Our dataset indicate that the deforestation emissions footprint is increasing in most regions worldwide. Notably, the higher the income level, the more deforestation emissions are hidden in international trade. Additionally, consumption-driven deforestation emissions from lower-income countries to higher-income countries also on the rise. While this study uses spatially detailed data to address some data deficiencies, uncertainties persist, particularly regarding the proportion of exports from each region. To improve these datasets in future work, more detailed supply chain data will be necessary.

## Author contribution

**Dongmei Tang:** Conceptualization, Methodology, Software, Formal analysis, Visualization, Writing - Original Draft.

**Yuanzhi Yao:** Conceptualization, Writing - Review & Editing, Funding acquisition. **Xia Li:** Conceptualization, Writing - Review & Editing, Supervision, Funding acquisition.

## 360 Competing interests

One of the authors of this manuscript, Yuanzhi Yao, is a member of the editorial board of the journal.

## Acknowledgements

This study was supported by the Key National Natural Science Foundation of China (Grant No. 42130107) and the National Natural Science Foundation of China (Grant No. 42371410).

## 365 References

Cook-Patton, S. C., Leavitt, S. M., Gibbs, D., Harris, N. L., Lister, K., Anderson-Teixeira, K. J., Briggs, R. D., Chazdon, R. L., Crowther, T. W., Ellis, P. W., Griscom, H. P., Herrmann, V., Holl, K. D., Houghton, R. A., Larrosa, C., Lomax, G., Lucas, R., Madsen, P., Malhi, Y., Paquette, A., Parker, J. D., Paul, K., Routh, D., Roxburgh, S., Saatchi, S., van den Hoogen, J.,



- Walker, W. S., Wheeler, C. E., Wood, S. A., Xu, L., and Griscom, B. W.: Mapping carbon accumulation potential from global natural forest regrowth, *Nature*, 585, 545-550, 10.1038/s41586-020-2686-x, 2020.
- 370 Curtis, P. G., Slay, C. M., Harris, N. L., Tyukavina, A., and Hansen, M. C.: Classifying drivers of global forest loss, *Science*, 361, 1108-1111, 10.1126/science.aau3445, 2018.
- DeFries, R. S., Rudel, T., Uriarte, M., and Hansen, M.: Deforestation driven by urban population growth and agricultural trade in the twenty-first century, *Nat Geosci*, 3, 178-181, 10.1038/ngeo756, 2010.
- 375 FAO: Global forest resources assessment 2015: how are the world's forests changing? , FAO, Rome, 2015.
- FAO: The State of the World's Forests 2020. Forests, biodiversity and people, FAO, Rome, <https://doi.org/10.4060/ca8642zh>, 2020.
- Friedlingstein, P., O'Sullivan, M., Jones, M. W., Andrew, R. M., Bakker, D. C. E., Hauck, J., Landschützer, P., Le Quéré, C., Lujckx, I. T., Peters, G. P., Peters, W., Pongratz, J., Schwingshackl, C., Sitch, S., Canadell, J. G., Ciais, P., Jackson, R. B., Alin, S. R., Anthoni, P., Barbero, L., Bates, N. R., Becker, M., Bellouin, N., Decharme, B., Bopp, L., Brasika, I. B. M., Cadule, P., Chamberlain, M. A., Chandra, N., Chau, T.-T.-T., Chevallier, F., Chini, L. P., Cronin, M., Dou, X., Enyo, K., Evans, W., Falk, S., Feely, R. A., Feng, L., Ford, D. J., Gasser, T., Ghattas, J., Gkritzalis, T., Grassi, G., Gregor, L., Gruber, N., Gürses, Ö., Harris, I., Hefner, M., Heinke, J., Houghton, R. A., Hurtt, G. C., Iida, Y., Ilyina, T., Jacobson, A. R., Jain, A., Jarníková, T., Jersild, A., Jiang, F., Jin, Z., Joos, F., Kato, E., Keeling, R. F., Kennedy, D., Klein Goldewijk, K., Knauer, J., 385 Korsbakken, J. I., Körtzinger, A., Lan, X., Lefèvre, N., Li, H., Liu, J., Liu, Z., Ma, L., Marland, G., Mayot, N., McGuire, P. C., McKinley, G. A., Meyer, G., Morgan, E. J., Munro, D. R., Nakaoka, S.-I., Niwa, Y., O'Brien, K. M., Olsen, A., Omar, A. M., Ono, T., Paulsen, M., Pierrot, D., Pockock, K., Poulter, B., Powis, C. M., Rehder, G., Resplandy, L., Robertson, E., Rödenbeck, C., Rosan, T. M., Schwinger, J., Séférian, R., Smallman, T. L., Smith, S. M., Sospedra-Alfonso, R., Sun, Q., Sutton, A. J., Sweeney, C., Takao, S., Tans, P. P., Tian, H., Tilbrook, B., Tsujino, H., Tubiello, F., van der Werf, G. R., van 390 Ooijen, E., Wanninkhof, R., Watanabe, M., Wimart-Rousseau, C., Yang, D., Yang, X., Yuan, W., Yue, X., Zaehle, S., Zeng, J., and Zheng, B.: Global Carbon Budget 2023, *Earth System Science Data*, 15, 5301-5369, 10.5194/essd-15-5301-2023, 2023.
- Friis, C. and Nielsen, J. Ø.: Telecoupling: Exploring land-use change in a globalised world, *Palgrave Studies in Natural Resource Management*, Springer, Switzerland 2019.
- Hansen, M. C., Potapov, P. V., Moore, R., Hancher, M., Turubanova, S. A., Tyukavina, A., Thau, D., Stehman, S. V., Goetz, S. J., Loveland, T. R., Kommareddy, A., Egorov, A., Chini, L., Justice, C. O., and Townshend, J. R.: High-resolution global maps of 21st-century forest cover change, *Science*, 342, 850-853, 10.1126/science.1244693, 2013.
- Harris, N. L., Gibbs, D. A., Baccini, A., Birdsey, R. A., de Bruin, S., Farina, M., Fatoyinbo, L., Hansen, M. C., Herold, M., Houghton, R. A., Potapov, P. V., Suarez, D. R., Roman-Cuesta, R. M., Saatchi, S. S., Slay, C. M., Turubanova, S. A., and Tyukavina, A.: Global maps of twenty-first century forest carbon fluxes, *Nat Clim Chang*, 11, 234-240, 10.1038/s41558-020- 400 00976-6, 2021.
- He, K., Mi, Z., Coffman, D. M., and Guan, D.: Using a linear regression approach to sequential interindustry model for time-lagged economic impact analysis, *Structural Change and Economic Dynamics*, 62, 399-406, <https://doi.org/10.1016/j.strueco.2022.03.017>, 2022.
- Henders, S., Persson, U. M., and Kastner, T.: Trading forests: land-use change and carbon emissions embodied in production and exports of forest-risk commodities, *Environ Res Lett*, 10, 10.1088/1748-9326/10/12/125012, 2015.
- 405 Hoang, N. T. and Kanemoto, K.: Mapping the deforestation footprint of nations reveals growing threat to tropical forests, *Nat Ecol Evol*, 5, 845-853, 10.1038/s41559-021-01417-z, 2021.
- Hong, C., Zhao, H., Qin, Y., Burney, J. A., Pongratz, J., Hartung, K., Liu, Y., Moore, F. C., Jackson, R. B., Zhang, Q., and Davis, S. J.: Land-use emissions embodied in international trade, *Science*, 376, 597-603, 10.1126/science.abj1572, 2022.
- 410 Hosseiny, B., Zaboli, M., and Homayouni, S.: Forest Change Mapping using Multi-Source Satellite SAR, Optical, and LiDAR Remote Sensing Data, *ISPRS Annals of the Photogrammetry, Remote Sensing and Spatial Information Sciences*, 163-168, 10.5194/isprs-annals-X-4-2024-163-2024, 2024.
- Kanemoto, K., Moran, D., and Hertwich, E. G.: Mapping the Carbon Footprint of Nations, *Environ Sci Technol*, 50, 10512-10517, 10.1021/acs.est.6b03227, 2016.
- 415 Kastner, T., Erb, K.-H., and Nonhebel, S.: International wood trade and forest change: A global analysis, *Global Environ Chang*, 21, 947-956, 10.1016/j.gloenvcha.2011.05.003, 2011.
- Lambin, E. F., Gibbs, H. K., Heilmayr, R., Carlson, K. M., Fleck, L. C., Garrett, R. D., le Polain de Waroux, Y., McDermott, C. L., McLaughlin, D., Newton, P., Nolte, C., Pacheco, P., Raush, L. L., Streck, C., Thorlakson, T., and Walker, N. F.: The



- role of supply-chain initiatives in reducing deforestation, *Nat Clim Chang*, 8, 109-116, 10.1038/s41558-017-0061-1, 2018.
- 420 Lenzen, M., Moran, D., Kanemoto, K., and Geschke, A.: Building Eora: a global multi-region input-output database at high country and sector resolution, *Econ Syst Res*, 25, 20-49, 10.1080/09535314.2013.769938, 2013.
- Lenzen, M., Sun, Y.-Y., Faturay, F., Ting, Y.-P., Geschke, A., and Malik, A.: The carbon footprint of global tourism, *Nat Clim Chang*, 8, 522-528, 10.1038/s41558-018-0141-x, 2018.
- 425 Liu, W., Zhang, X., Zhao, T., Wang, J., Li, Z., and Liu, L.: Revealing the proximate drivers behind global tree cover loss using multisourced remote sensing products during 2000–2020, *Forest Ecol Manag*, 579, 10.1016/j.foreco.2025.122501, 2025.
- Liu, X., Zhang, J., Zhang, H., Tang, D., Hu, G., and Li, X.: China's Mismatch of Public Awareness and Biodiversity Threats under Economic Trade, *Environ Sci Technol*, 56, 9784-9796, 10.1021/acs.est.2c00844, 2022.
- 430 Meijer, J. R., Huijbregts, M. A. J., Schotten, K. C. G. J., and Schipper, A. M.: Global patterns of current and future road infrastructure, *Environ Res Lett*, 13, 10.1088/1748-9326/aabd42, 2018.
- Moran, D., Giljum, S., Kanemoto, K., and Godar, J.: From Satellite to Supply Chain: New Approaches Connect Earth Observation to Economic Decisions, *One Earth*, 3, 5-8, 10.1016/j.oneear.2020.06.007, 2020.
- Pendrill, F., Persson, U. M., Godar, J., and Kastner, T.: Deforestation displaced: trade in forest-risk commodities and the prospects for a global forest transition, *Environ Res Lett*, 14, 055003, 10.1088/1748-9326/ab0d41, 2019a.
- 435 Pendrill, F., Persson, U. M., Godar, J., Kastner, T., Moran, D., Schmidt, S., and Wood, R.: Agricultural and forestry trade drives large share of tropical deforestation emissions, *Global Environ Chang*, 56, 1-10, 10.1016/j.gloenvcha.2019.03.002, 2019b.
- Souza Jr, C.: Assessing the scale of rubber deforestation in southeast Asia, *Nature*, 623, 256-257, 10.1038/d41586-023-03153-9, 2023.
- 440 Sun, Z., Scherer, L., Tukker, A., and Behrens, P.: Linking global crop and livestock consumption to local production hotspots, *Global Food Security*, 25, 100323, 10.1016/j.gfs.2019.09.008, 2020.
- Tang, D., Yao, Y., and Li, X.: Consumption-based Carbon Emissions for Deforestation (2001–2015), figshare [dataset], <https://doi.org/10.6084/m9.figshare.28091879.v2>, 2024.
- 445 Tang, D., Li, X., Xu, X., Liu, X., Zhang, H., Shi, H., Liu, S., and Zhang, H.: Does the Belt and Road Initiative Really Increase CO<sub>2</sub> Emissions?, *Ann Am Assoc Geogr*, 112, 948-967, 10.1080/24694452.2021.1941747, 2021.
- Verburg, P. H., Ellis, E. C., and Letourneau, A.: A global assessment of market accessibility and market influence for global environmental change studies, *Environmental Research Letters*, 6, 034019, 2011.
- 450 Wang, Y., Hollingsworth, P. M., Zhai, D., West, C. D., Green, J. M. H., Chen, H., Hurni, K., Su, Y., Warren-Thomas, E., Xu, J., and Ahrends, A.: High-resolution maps show that rubber causes substantial deforestation, *Nature*, 623, 340-346, 10.1038/s41586-023-06642-z, 2023.
- Wiedmann, T. and Lenzen, M.: Environmental and social footprints of international trade, *Nat Geosci*, 11, 314-321, 10.1038/s41561-018-0113-9, 2018.
- Yang, Y., Qu, S., Cai, B., Liang, S., Wang, Z., Wang, J., and Xu, M.: Mapping global carbon footprint in China, *Nat Commun*, 11, 2237, 10.1038/s41467-020-15883-9, 2020.

455